Insights for Light-Driven Molecular Devices from *Ab Initio* Multiple Spawning Excited-State Dynamics of Organic and Biological Chromophores

TODD J. MARTíNEZ*
Department of Chemistry, Beckman Institute, and The Frederick Seitz Materials Research Laboratory, University of Illinois, 600 S. Mathews Avenue, Urbana, Illinois 61801

Received May 2, 2005

ABSTRACT
We discuss the basic process of photoinduced isomerization as a building block for the design of complex, multifunctional molecular devices. The excited-state dynamics associated with isomerization is detailed through application of the *ab initio* multiple spawning (AIMS) method, which solves the electronic and nuclear Schrödinger equations *simultaneously*. This first-principles molecular dynamics approach avoids the uncertainties and extraordinary effort associated with fitting of potential energy surfaces and allows for bond rearrangement processes with no special input. Furthermore, the AIMS method allows for the breakdown of the Born−Oppenheimer approximation and thus can correctly model chemistry occurring on multiple electronic states. We show that charge-transfer states play an important role in photoinduced isomerization and argue that this provides an essential "design rule" for multifunctional devices based on isomerizing chromophores.

Introduction

The design of functional molecular architectures has emerged as one of the major goals of chemistry in the past decade, as evidenced by three recent special issues of this journal.[1−3] With the advent of modern lasers, it is now possible to simultaneously control spatial and temporal characteristics of light at a level that approaches natural molecular length (nanometer) and time (femtosecond) scales. Carefully designed optically responsive molecules can be envisioned as a means to transfer this detailed control to molecular transport and function. We are not talking primarily about "active" control schemes in this context, where the detailed time-frequency profile of a laser pulse is optimized to drive a particular chemical reaction.[4,5] Rather, we are thinking of molecules that behave as devices, containing one or more optically addressable components surrounded by a scaffolding. The scaffolding must protect the chromophores, but it also should direct their photodynamics and amplify the effects of any photochemical transformation.

The simplest examples would be optically responsive polymers that might transform optical signals into mechanical work. Such examples have been reported recently, building on the photoinduced cis−trans isomerization of azobenzene. Incorporating azobenzene into polymers, Hugel et al. were able to demonstrate the use of light to power mechanical work in the form of motion of an atomic force microscope (AFM) tip.[6] In a similar study, Yu et al. showed how azobenzene-containing polymer films can be curled and uncurled by exposure to light.[7] Interestingly, they also showed that the laser polarization can be used as an additional variable to control the direction along which the film curls. It is not difficult to see how the kind of behavior shown in these examples could be exploited on a larger scale. However, they fall short of being molecular devices. The behavior of the chromophoric unit is not substantially modified by the surrounding environment, and there is no obvious mechanism to endow the systems with multifunctional character, where molecular function can be controlled by pulse sequencing.

Much closer to the devices that we envision in terms of nascent complexity are photoactive proteins. A selection of three such proteins that have been of interest in our group is shown in Figure 1. Bacteriorhodopsin (bR) is a light-driven ion pump, unidirectionally pumping protons across a membrane after the retinal-protonated Schiff base (henceforth referred to as retinal) chromophore photoisomerizes. The protein environment provides the "water wires" that connect the intra- and extracellular regions to the chromophoric element. Thus, the protein environment may be considered as an amplifier, converting the angstrom-scale motion of retinal induced by light absorption into directed motion over more than 30 Å across the membrane. The photoactive yellow protein (PYP) is the active element in negative phototaxis of *Ectothiorhodospira halophila* bacteria, responsible for initiating the signaling cascade that leads the bacteria to avoid blue light. Again, isomerization of a chromophore (*p*-coumaric acid) is the initial step, but in this case, isomerization induces a conformational change of the protein that initiates a cascade of events culminating in the modification of flagellar motion. Thus, the entire organism plays a critical role in an amplification process that extends from several angstroms (isomerization of the PYP chromophore) to microns (swimming of the bacteria). The green fluorescent protein (GFP) is interesting in that it uses a chromophore that is chemically very similar to that in PYP, but the function of the protein hinges on *preventing* isomerization. Instead, GFP acts as a wavelength converter, absorbing blue light and emitting green light. All three of these proteins have mesoscale functions that are triggered by light aborption that is directly responsible for subsequent chemical changes on small-length scales. The

Todd Martinez was born in 1968 in Amityville, NY, and was raised in Central America and the Carribbean. He returned to the U.S. to complete his undergraduate education at Calvin College. After doctoral studies at UCLA and postdoctoral research at UCLA and Hebrew University, he began his independent career in 1996 at the University of Illinois. His research interests focus on the quantum chemistry and dynamics of electronically excited states in organic, inorganic, and biological molecules and on the development of first-principles molecular dynamics methods including quantum mechanical effects.

* To whom correspondence should be addressed. Telephone: 217-333-1449. Fax: 217-244-3186. E-mail: tjm@spawn.scs.uiuc.edu.

10.1021/ar040202q CCC: $33.50
Published on Web 10/12/2005

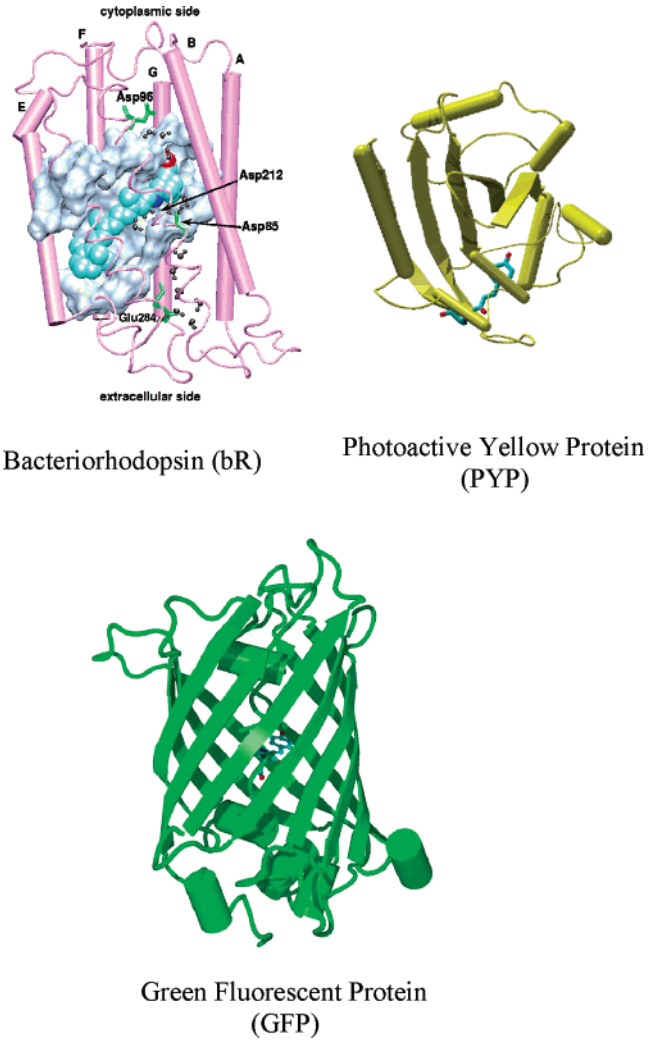

FIGURE 1. Three photoactive proteins that can be considered as rudimentary molecular devices. bR is membrane-bound, while PYP and GFP are aqueous.

protein directs the resulting behavior of the chromophore and amplifies it in a particular way to achieve the desired function. These functionalities are strikingly different, ranging from chemically and directionally specific transport to signaling and wavelength conversion. There has been no evolutionary driving force to persuade biological systems to exploit fine-scale spatio-temporal characteristics of light, because they are always presented with essentially continuous, broadband radiation. However, there is also nothing to prevent the adoption of these systems in such a context.

One might think that the diversity of functionality present in photobiological systems is simply a consequence of the distinct chromophoric units. This scenario is easily dismissed by a comparison of the behavior of various chromophores in solution and protein environments. For example, illumination of the all-*trans* retinal chromophore in solution leads to a mixture of isomerized products, with the dominant one being isomerization about the C_{11}=C_{12} bond.[8] The quantum yield for photoisomerization is 20%, and the time scale for photoisomerization is greater than 10 ps.[9] In the bR protein environment, the only photoisomerization product is *cis* about the C_{13}=C_{14} bond, the isomerization quantum yield exceeds 60%, and the time scale for photoisomerization is subpicosecond.[10] Thus, the protein environment acts to sharpen the product distribution (about one of the minor products!) and to simultaneously increase both the reaction rate and efficiency. This combination of effects alone is quite interesting. It is easy to conceive of steric effects that block one or more of the possible reaction pathways, thus sharpening the product distribution. However, in general, this would be expected to lead to a decreased quantum yield because more of the photon energy would be lost to heat by molecules that happened to attempt to produce one of the disfavored products. Furthermore, it would not be expected to significantly affect the reaction time scale. A similar example is found in GFP, where chromophore analogues exhibit little fluorescence in solution above cryogenic temperatures[11] but have a fluorescence quantum yield exceeding 60% in the protein environment.[12] Clearly, the protein environment plays a major role in altering the excited state reactivity of the chromophore and should not be viewed as merely a "molecular-scale beaker". Thus, the first goal in designing light-driven devices should be a detailed understanding of the nascent behavior of the isolated chromophore and the "design rules" by which the protein environment alters chromophore dynamics.

Ab Initio Multiple Spawning (AIMS)

The AIMS method has been developed to carry out first-principles simulations of chemical reaction dynamics including quantum effects. The primary emphasis thus far has been on reactions involving electronically excited states, where the breakdown of the Born−Oppenheimer approximation, i.e., "surface crossing," must be properly treated. We provide only a brief summary highlighting the important features of the method, as detailed reviews exist in the literature.[13,14] The AIMS method is designed to simulate quantum dynamics *without* prior knowledge of the potential energy surfaces (PESs) or their nonadiabatic couplings (which promote transitions between electronic states). An immediate problem is the global nature of the nuclear Schrödinger equation (the entire PES is required at each time step) compared to the local nature of quantum chemistry that comes from the underlying Born−Oppenheimer approximation (energies and gradients are only evaluated at one nuclear configuration at a time). We circumvent this problem by representing the nuclear wave function in a semilocal basis set of complex frozen Gaussians.[15] While these basis functions are not completely localized (they have a position-momentum uncertainty as required by Heisenberg's uncertainty principle), they are sufficiently localized that approximation schemes can be introduced to evaluate the required integrals over the PESs and their couplings. The basis functions are associated with complex coefficients whose time evolution is determined by the nuclear Schrödinger equation. The centers of the basis functions themselves

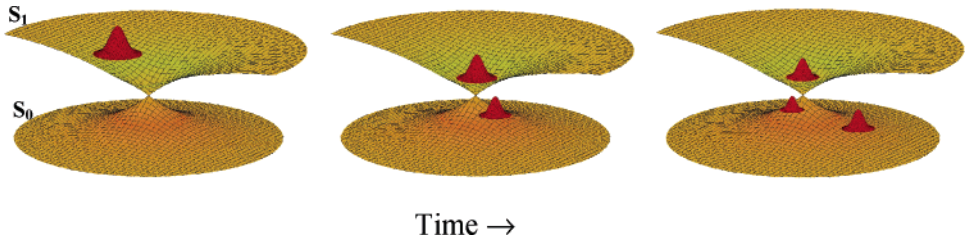

FIGURE 2. Schematic description of the multiple spawning method. The nuclear wave function is represented as a superposition of Gaussian wave packets, and the basis set increases as nonadiabatic regions are encountered (like the conical intersection shown here). The Gaussian basis functions follow classical trajectories. The population (indicated schematically by the heights of the Gaussian wave packets) is transferred between trajectory basis functions by the solution of the nuclear Schrödinger equation, which couples all of the basis functions. In the AIMS method, the potential energy surfaces are calculated simultaneously with the dynamical evolution, as needed.

move along classical trajectories, and an adaptive basis set expansion technique ("spawning") is used to account for quantum effects such as tunneling and electronic curve crossing. The method is shown in schematic form in Figure 2. This figure also provides a picture of a conical intersection, a true degeneracy of two adiabatic electronic states. These conical intersections are now known to play a major role in nonradiative decay from excited electronic states[16−18] and bear a certain resemblance to transition states in ground-state chemical reactions. As time progresses in Figure 2, the initial basis function (starting on the upper electronic state) approaches a conical intersection. New basis functions are introduced ("spawned") on the lower electronic state as needed. The nuclear Schrödinger equation is solved in this time-evolving, nonorthogonal basis set and thus dictates the fraction of the population associated with each of the basis functions. Figure 2 emphasizes the description of the multiple spawning aspects of the nuclear dynamics. It does not provide a good sense of the fact that, in AIMS, the electronic Schrödinger equation is being solved simultaneously; therefore, the PESs and their gradients are only known at a few points at any given time.

Ethylene—Paradigm for Photoinduced *cis*−*trans* Isomerization

The textbook picture of photoinduced *cis*−*trans* isomerization[19] is largely based on torsion as the reaction coordinate. Torsion is favored on the excited electronic state because of both electronic kinetic energy and Coulombic repulsion effects. Importantly, the energy gap between the lowest singlet excited electronic state and the ground state at a rigidly twisted geometry is greater than 1 eV in ethylene. This remains true even if one allows for relaxation of C−H bond lengths and ∠HCH bond angles and for any reasonable electronic structure method, e.g., complete active space self-consistent field[20] (CASSCF), multireference configuration interaction (MRCI), or perturbation-theory corrected CASSCF[21] (CASPT2). The difficulty with this finding in the context of the conventional photochemical mechanism is that the electronic relaxation in small conjugated molecules is known to be very fast, on the order of a few hundred femtoseconds. However, the rate of electronic curve crossing in the presence of such a large gap (greater than 1 eV) would certainly exceed picosecond time scales. Of course, the large S_0/S_1 gap after torsional relaxation does not preclude a smaller gap after further relaxation. As one might anticipate from the foregoing discussion, there is a conical intersection involved at a geometry that requires further distortion of the molecule. Our previous AIMS simulations have shown that the electronic quenching is complete in somewhat less than 200 fs and that a minimal model for the photoisomerization mechanism must include both torsion and pyramidalization (sp^3 hybridization) about one of the carbon atoms.[14,22−24] These two distortions figure prominently in the minimal energy conical intersection (MECI) geometry of ethylene.

Pyramidalization reflects the stabilization of a zwitterionic $H_{22}C{=}CH^+$ structure that is strongly reminiscent of the "sudden polarization" ideas advanced by Salem.[25] However, the "suddenness" is not particularly important here, and it was not previously recognized that the minimal energy point on S_1 was a conical intersection. The charge-transfer character involved in the excited-state dynamics is clearly evident in Figure 3, where we show the natural orbitals of the electronic wave function (MRCI) along the center of a representative trajectory basis function. Furthermore, the electronic character switches from zwitterionic to covalent and back again during the dynamics. The PESs shown in the left panel of Figure 4 make the origin of this behavior clear; the excited-state surface has four symmetry-equivalent wells corresponding to pyramidalization up or down for the left or right carbon atom (only two of these wells, corresponding to pyramidalization of the left and right carbon atoms, are shown because of graphical constraints). Figure 4 shows adiabatic potential energy surfaces, and consequently, the electronic character can be different at different points along the excited-state surface. In comparison with Figure 3, one can determine that the electronic character is charge-transfer-like (doubly occupied orbital localized on one of the carbon atoms) near the twisted and pyramidalized geometries that characterize the excited-state "minima", while the electronic character is more like a single excitation ($\pi \rightarrow \pi^*$) in the Franck−Condon region.

In the right panel of Figure 4, we show the effect of a surrounding point charge. Because the pyramidalized carbon atom is negatively charged, a surrounding positive point charge biases the photochemical mechanism such that pyramidalization about the carbon closest to the point charge is favored. In the context of ethylene, this is

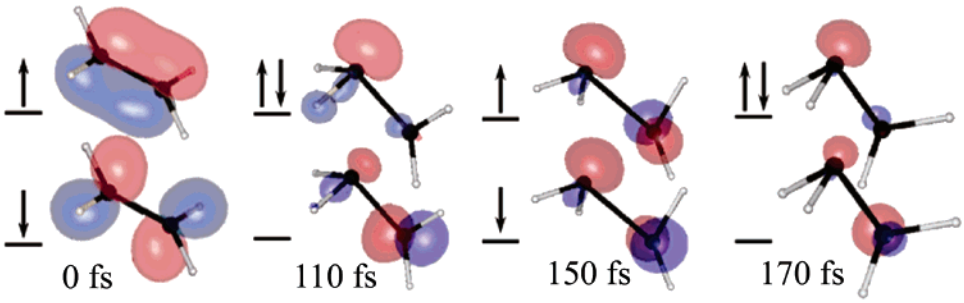

FIGURE 3. Snapshots of the π and π^* natural orbitals during a representative AIMS simulation of ethylene photodynamics. The occupation number (rounded to the nearest integer) of each orbital is indicated by the arrows on the energy level diagram to the left of each snapshot. The intramolecular electron-transfer character of the excited-state dynamics is evident as well as the pronounced pyramidalization about one of the carbon atoms.

not particularly fruitful; the final products resulting from pyramidalization of the left and right carbon atoms are indistinguishable. However, such is no longer the case when the ethylene molecule is appropriately substituted or, more importantly, when there are multiple bonds about which isomerization can occur.

A critical reader might ask at this point whether there is any evidence that the AIMS procedure is sufficiently accurate. Certainly, there are approximations that might be important in certain cases. For example, there is limited accounting of wave packet spreading because the nuclear basis functions are of the frozen Gaussian form. Spreading of the wave packet can be described by population transfer between basis functions on the same electronic surface, and such effects are observed. However, a complete description of this effect would require very large nuclear basis sets. Similarly, the electronic structure treatment itself is necessarily less accurate than what could be employed in locating stationary points such as excited-state minima or MECI geometries. For this reason, it is important to note that we use an iterative procedure for AIMS simulations where the dynamics at a given level of theory is validated by characterization of the potential energy surfaces using a higher level of theory. The best quantitative assessment of the expected accuracy of the method is thus obtained by direct comparison to experiments. We do not go into details here but simply point out some previous results.

The AIMS results for photoisomerization of ethylene have been compared to pump-photoionization probe measurements to arrive at a predicted signal lifetime[14] of 30 fs, compared to the experimentally observed[26] 30 ± 15 fs. In this case, it was particularly important to model the experimental signal directly, because the observed lifetime does not correspond to the time when the wave packet is on the S_1 excited state (the wave packet leaves the ionization region while still on the S_1 excited state). We have also exploited the fact that nuclear wave functions are available in AIMS to compute electronic absorption spectra of ethylene, again in good agreement with the experiment.[27,28] Further comparisons for other molecules have been described in the literature, and more are underway. Finally, we have investigated the ground- and excited-state PESs of ethylene using more accurate electronic structure methods including dynamic electron correlation effects[23,28] The essential features of the PESs as emphasized above are robust to improvements in the quantum chemical treatment.

The further question that one is naturally inclined to ask is whether the importance of the charge-transfer state and pyramidalization of a carbon atom are generic in photoisomerization or whether these are instead specific to ethylene. Investigation of a variety of other isomerizing molecules such as stilbene and the GFP and PYP chromophores supports the idea that these are generic features.[29−31] One notable difference is that the absolute minimum on the lowest singlet excited state is *not* a conical intersection in these cases, as it is in ethylene. This has significant consequences as detailed for GFP chromophore below. Furthermore, calculations of MECI geometries in retinal show no evidence for pyramidalization.[32] Nevertheless, charge transfer is also an important component of the electronic states involved at the MECI in retinal. The coordinate that tunes the energy of the charge-transfer state in retinal is C=N stretching instead of pyramidalization. This can be expected on chemical grounds; the important feature for all of the isomerizing molecules that we have discussed is that access to a charge-transfer state is required to reach low-energy conical intersections connecting the ground and excited states. When heteroatoms are present, it is not surprising that the preferred distortion that accomplishes stabilization of the charge-transfer excited state is no longer pyramidalization of a carbon atom but instead involves relative motion of atoms with differing electronegativity.

The connection between charge-transfer states, MECI geometries, and surrounding point charges is also made clear by searching for MECIs in a retinal analogue in the presence of the Cl^- anion. The results are shown in Figure 5, for two MECIs involving twisting about the C_{11}=C_{12} and C_{13}=C_{14} bonds. The Cl^- counterion follows the isomerization, or equivalently, if the Cl^- counterion were fixed, it would bias the excited-state reaction path to twist about the closest isomerizable bond. Indeed, inspection of the X-ray structures for bR[33] and rhodopsin[34] indicates in both cases the presence of two ionized residues, not involved in salt bridges, near the retinal chromophore: Asp85/Asp212 and Glu113/Glu181 for bR and rhodopsin, respectively. In both proteins, one of these (Asp85/Glu113) is closest to the proton of retinal (mediated by a hydrogen-

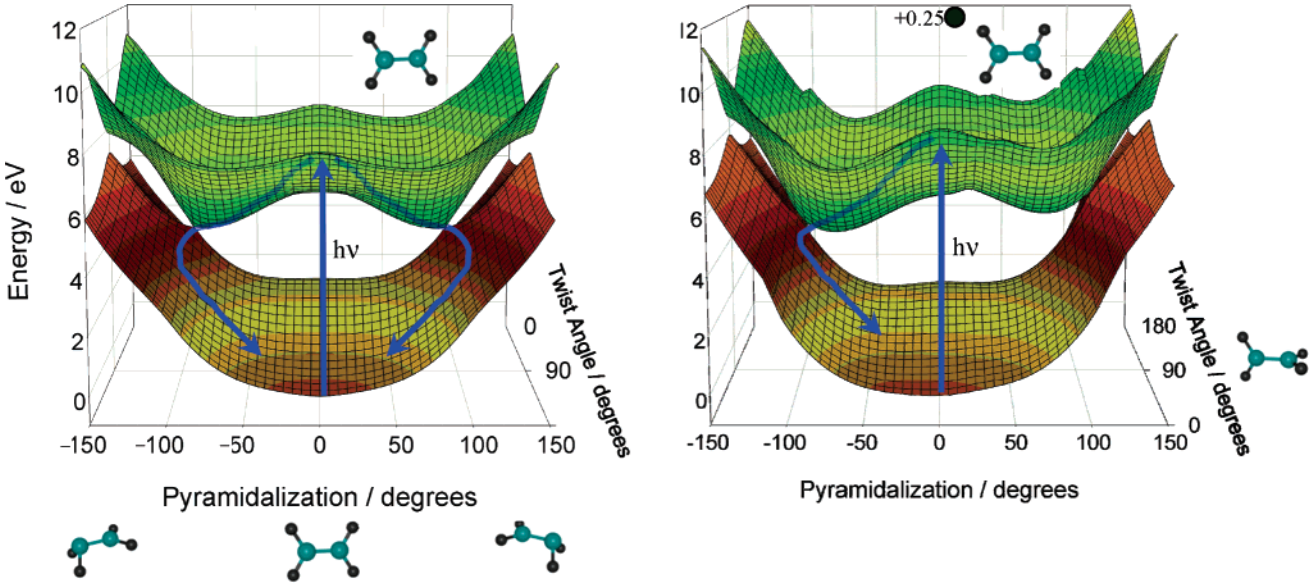

FIGURE 4. Ground- and excited-state potential energy surfaces for isolated ethylene (top) and ethylene in the field of a point charge (bottom), computed with a state-averaged CASSCF(2/2) wave function. The photoisomerization mechanism is schematically indicated with arrows and in both cases involves twisting about the C=C bond and pyramidalization of one of the carbon atoms. Positive and negative pyramidalization angles indicate pyramidalization of the left or right carbon atoms, respectively. The presence of a positive point charge (3 Å away from the left carbon atom) leads to stabilization of one of the charge-transfer states and biases the photoisomerization mechanism such that the left carbon atom is more likely to pyramidalize.

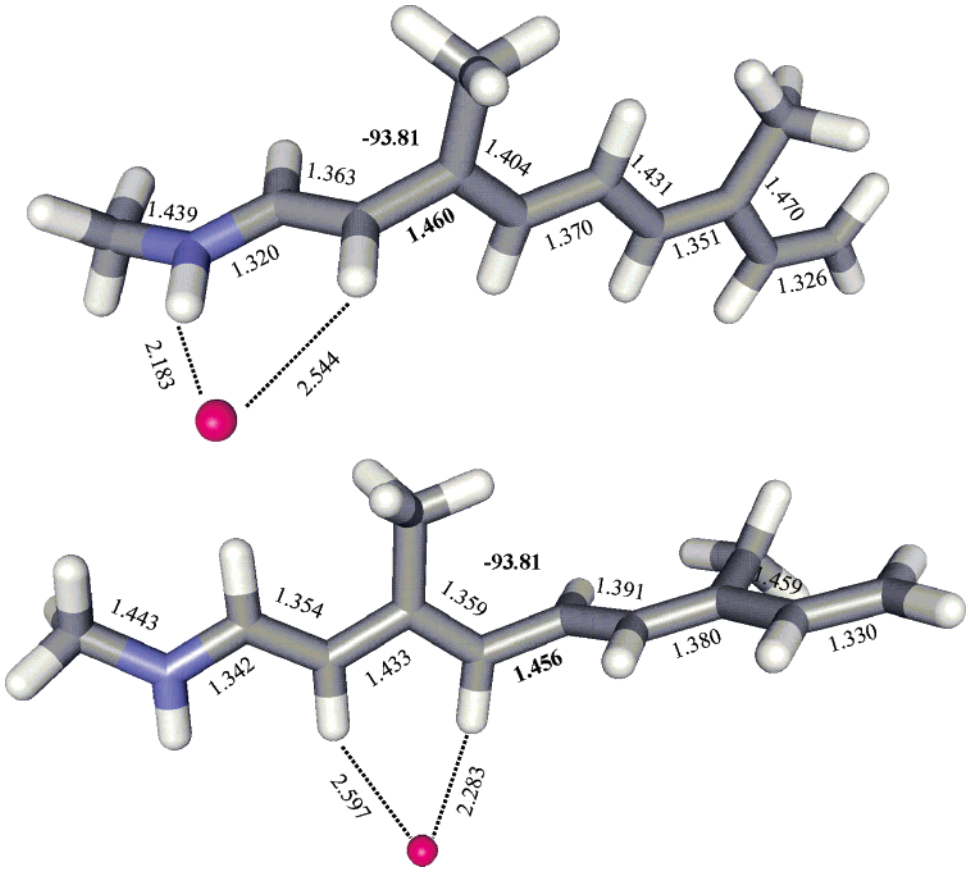

FIGURE 5. Optimized S_1/S_0 MECI geometries for a retinal chromophore analogue surrounded by a Cl^- point charge (magenta). The SA-2-CASSCF(10/10) method was used with a 6-31G* basis set. Bond lengths (Å) are shown, with the bond length and dihedral angle associated with the isomerized bond in bold. Notice that the lowest energy MECI is twisted about the bond closest to the Cl^- anion.

bonded crystallographic water molecule in bR) and the other (Asp212/Glu181) is closest to the bond about which retinal photoisomerizes (C_{13}=C_{14} in bR and C_{11}=C_{12} in rhodopsin). One can speculate that one of the ionized residues plays a role as a counterion for the protonated Schiff base and that the other plays a role in tuning bond

selectivity. Interestingly, the dark-adapted form of retinal in rhodopsin is 11-*cis*, implying that isomerization would occur around C_{11}=C_{12} even in the absence of a tuning charge. Nevertheless, the surrounding ionized residue is predicted to accelerate the reaction and enhance the quantum yield for isomerization.

"Nearly" *Ab Initio* Multiple Spawning

To investigate the role of condensed phase and/or protein environments in photoisomerization dynamics, it is currently necessary to invoke some approximations beyond those in AIMS. Specifically, we must be able to compute ground- and excited-state PESs many times if we are to follow the dynamical evolution. It is not currently feasible to calculate the excited-state energy of a protein for even a single geometry with *ab initio* methods, much less the many thousands that are necessary for AIMS. To extend our simulations beyond isolated molecules, we use a combination of reparametrized multireference semiempirical and hybrid quantum mechanical/molecular mechanical (QM/MM) methods. Semiempirical methods, such as AM1,[35] have a long history in chemistry but have primarily been parametrized and used for ground electronic states. These methods use minimal valence basis sets, neglect some of the two-electron integrals, and parametrize other integrals. However, they retain a wavefunction-based picture, and thus, it should not be surprising that many concepts from *ab initio* quantum chemistry are applicable. For example, the multireference character of the electronic wave function is necessary for accurate depiction of the PESs around conical intersections because there are at least two electronic states that are exactly degenerate at these points. Thus, we use a modified semiempirical method that is intended to mimic state-averaged CASSCF as closely as possible. Static electron correlation (near-degeneracy) effects are thus treated directly. The parametrization of the integrals is adjusted by direct comparison to *ab initio* methods for a given molecule. If it is possible to model the effects of dynamic electron correlation through the semiempirical parametrization, this procedure can be expected to be quite accurate. In a number of molecules, we have found this to be the case. Our work thus far has adjusted the parameters for each different molecule, but we are also investigating the degree to which transferability can be achieved. An example of the kind of accuracy that can be achieved with few *ab initio* data points (electronic excitation energies at S_0 minima and relative energies of S_1/S_0 MECIs) is shown for the neutral form of the GFP chromophore in Figure 6. The improved semiempirical method is significantly closer to the *ab initio* CASPT2 results (which include both static and dynamic electron correlation effects) than state-averaged CASSCF. At the same time, the semiempirical method is at least an order of magnitude less computationally expensive than the CASSCF method (and more than 2 orders of magnitude less costly than CASPT2).

The QM/MM decomposition has been introduced nearly 3 decades ago[36] and has seen renewed interest in the last 10 years.[37] We will not go over the method in any great detail but simply state that the idea is to exploit the locality that is often observed in chemistry. In the case of photochemistry, there is usually a relatively small molecule (or part of a molecule) that is directly involved in the electronic excitation. If the influence of the surroundings is primarily described as a combination of steric and electrostatic effects, it can be modeled with an empirical force field such as CHARMM[38] or AMBER.[39] The chromophoric part of the molecule can then be modeled quantum mechanically, with either an *ab initio* or semiempirical wave function.

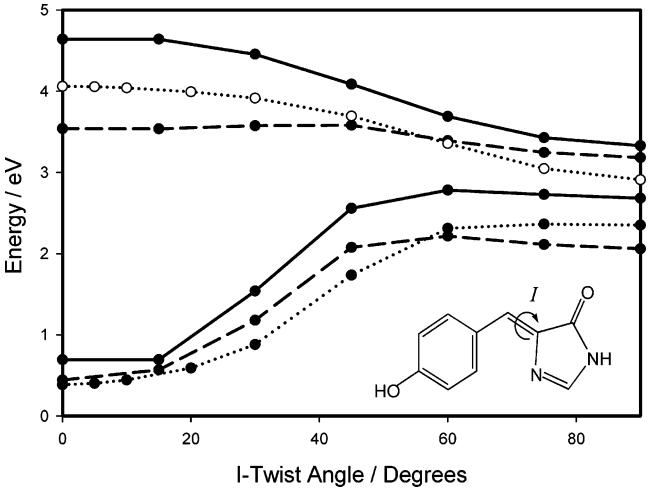

FIGURE 6. Comparison between reparametrized multireference semiempirical (•••) S_0 and S_1 PESs along S_1-coordinate-driving paths (optimizing all coordinates except for the indicated torsion angle on the S_1 PES) with the corresponding PESs from SA-2-CAS(2,2) (—) and CASPT2 (- - -). The semiempirical and CASSCF paths are optimized separately. The CASPT2 results are obtained along the CASSCF-optimized paths. The zero of energy is in all cases chosen to be the S_0 minimum at the respective level of theory.

GFP Chromophore—Influence of Aqueous Solvent

We have implemented the reparametrized multireference semiempirical method within a QM/MM context and interfaced this with multiple spawning dynamics.[29,40,41] We turn now to an example that illustrates the role of aqueous solvent, a disordered polarizable environment. We have carried out "nearly" AIMS simulations (using the improved semiempirical and QM/MM methods to generate the PESs and their couplings in place of more costly *ab initio* methods) of the excited-state dynamics in the neutral form of GFP chromophore (see the inset to Figure 6) after photoexcitation to the S_1 state. As mentioned in the Introduction, this chromophore is known not to fluoresce significantly in solution environments. However, the lifetime for fluorescence decay has been measured using ultrafast spectroscopy, and the dominant component was found to be 70 fs.[42]

In Figure 7, we show the results of "nearly" AIMS dynamics for the population on the excited electronic state in both the isolated molecule and in an aqueous environment (microsolvated cluster of 151 water molecules mod-

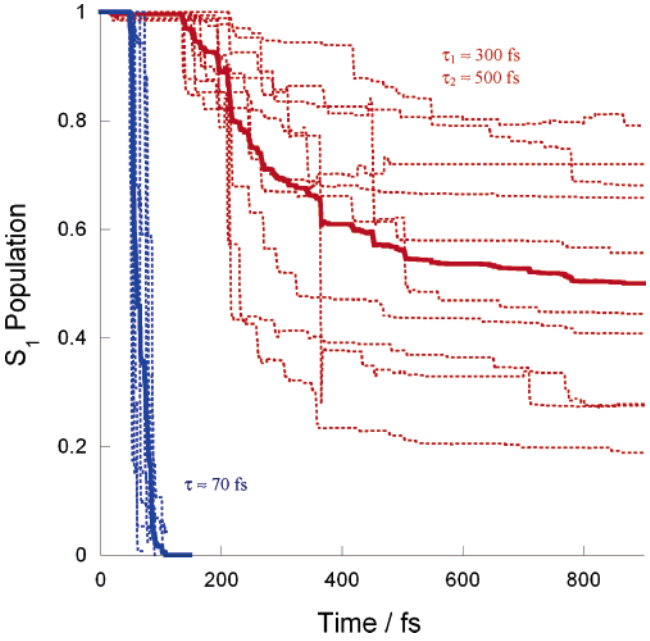

FIGURE 7. Excited-state population as a function of time for the neutral form of the GFP chromophore in vacuum (red) and microsolvated aqueous (blue) environments. The dotted lines refer to individual runs, and the dark lines represent the averaged behavior. Aqueous solvation dramatically decreases the excited-state lifetime.

eled with the SPC[43] force field). The difference in the excited-state lifetime is quite dramatic, with the aqueous environment accelerating the return to the ground state by at least an order of magnitude. This should not be unexpected in view of the comments made above. A polarizable environment can play the same role as a discrete charge in stabilizing the charge-transfer state and thus enabling access to the MECI that controls excited-state decay. This is shown in Figure 8, where we compare the ground- and excited-state energies at the minima on S_0 and S_1 and the S_0/S_1 MECI. Most important to note is that the S_0/S_1 MECI becomes the absolute minimum on S_1 upon solvation, while this MECI is roughly 0.3 eV above a twisted S_1 minimum in the isolated molecule. While one might be tempted to point out that the isolated molecule behaves more like the protein-bound chromophore than the solvated chromophore, this should be avoided. Although the excited-state lifetime is longer in both protein and vacuum compared to aqueous solution, the isolated chromophore will not fluoresce at all in the energy region where GFP fluoresces because the S_1 minimum is twisted. Note the S_0/S_1 gap at the S_1 minimum, which is 0.7 eV, corresponds to emission in the infrared (1.8 μm). The fluorescent geometry in the protein environment is almost certainly a planar form of the chromophore. It remains to be determined whether electrostatic effects also play a role in the stabilization of such a planar form and to what extent they also stabilize or destabilize the MECI, which would quench fluorescence.

Summary and Future Outlook

We have shown that a charge-transfer state forms the "doorway" to efficient radiationless decay in cis−trans

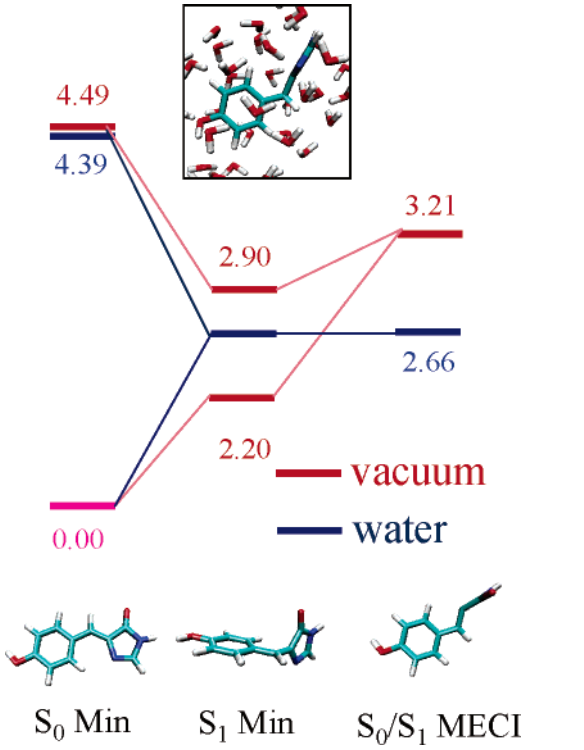

FIGURE 8. Effect of aqueous microsolvation on the energies (in eV) of important geometries in the photoisomerization of the neutral form of GFP chromophore. For the isolated chromophore, the twisted S_1 minimum geometry is distinct from the S_0/S_1 MECI and roughly 0.3 eV lower in energy. However, the S_0/S_1 MECI becomes the absolute minimum on S_1 after solvation.

isomerization. Thus, the outcome of the isomerization process can be controlled by tuning the surrounding electric field. We were able to understand this process in detail using the AIMS method, which avoids any preconceptions about the ground- and excited-state PESs and solves the nuclear and electronic Schrödinger equations simultaneously. Using QM/MM and reparametrized multireference semiempirical methods, we showed that it is possible to model excited-state dynamics for large chromophores in solvent and protein environments. One should be able to begin designing optomechanical systems using the insights that we have gained concerning the isomerization process. The ideal place to begin is by redesigning existing photoactive proteins. For example, one could predict mutations in GFP that would quench or enhance fluorescence. Alternatively, one could imagine mutated forms of bR that would isomerize about a different bond than usual. Looking further into the future, one could construct and introduce nonnatural amino acids that would create a dipolar field upon photoexcitation. If these were addressable separately from the chromophore (absorbing at different wavelengths), sequences of pulses could be designed that would lead to multifunctional behavior. Because of the flexibility of AIMS and the QM/MM extensions, we believe that purely computational design is now possible (provided that the mutations are not so severe as to render the folding of the protein questionable). It remains to prove this by

example, and work along these lines is currently underway.

I thank my co-workers over the past 5 years for their critical contributions to this work, especially M. Ben-Nun, L. Manohar, S. Olsen, J. Quenneville, and A. Toniolo. This work was supported by the National Science Foundation (CHE-02-311876 and BES-04-03846) with partial support from the Department of Energy through the Frederick Seitz Materials Research Laboratory (DOE DEFG02-91ER45439) at the University of Illinois Urbana-Champaign. T. J. M. is a Packard Fellow, MacArthur Fellow, and Dreyfus Teacher−Scholar. VMD has been used to generate some of the figures.[44]

References

(1) Reed, C. A. Molecular architectures. *Acc. Chem. Res.* **2005**, *38*, 215−216.
(2) Stoddart, J. F. Molecular machines. *Acc. Chem. Res.* **2001**, *34*, 410−411.
(3) Heath, J. R. Nanoscale materials. *Acc. Chem. Res.* **1999**, *32*, 388−389.
(4) Gordon, R. J.; Zhu, L.; Seideman, T. Coherent control of chemical reactions. *Acc. Chem. Res.* **1999**, *32*, 1007−1016.
(5) Rabitz, H.; Zhu, W. Optimal control of molecular motion: Design, implementation, and inversion. *Acc. Chem. Res.* **2000**, *33*, 572−578.
(6) Hugel, T.; Holland, N. B.; Cattani, A.; Moroder, L.; Seitz, M.; Gaub, H. E. Single-molecule optomechanical cycle. *Science* **2002**, *296*, 1103−1106.
(7) Yu, Y.; Nakano, M.; Ikeda, T. Photomechanics: Directed bending of a polymer film by light. *Nature* **2003**, *425*, 145.
(8) Freedman, K.; Becker, R. S. Comparative investigation of the photoisomerization of the protonated and unprotonated *n*-butylamine Schiff bases of 9-*cis*-, 11-*cis*-, 13-*cis*-, and all-*trans*-retinals. *J. Am. Chem.* Soc. **1986**, *108*, 1245−1251.
(9) Logunov, S. L.; Song, L.; El-Sayed, M. A. Excited-state dynamics of a protonated retinal Schiff base in solution. *J. Phys. Chem.* **1996**, *100*, 18586−18591.
(10) van der Horst, M. A.; Hellingwerf, K. J. Photoreceptor proteins, "star actors of modern times": A review of the functional dynamics in the structure of representative members of six different photoreceptor families. *Acc. Chem. Res.* **2004**, *37*, 13−20.
(11) Kojima, S.; Ohkawa, H.; Hirano, T.; Maki, S.; Niwa, H.; Ohashi, M.; Inouye, S.; Tsuji, F. I. Fluorescent properties of model chromophores of tyrosine-66 substituted mutants of aequorea green fluorescent protein (GFP). *Tetrahedron Lett.* **1998**, *39*, 5239−5242.
(12) Chattoraj, M.; King, B. A.; Bublitz, G. U.; Boxer, S. G. Ultra-fast excited-state dynamics in green fluorescent protein: Multiple states and proton transfer. *Proc. Natl. Acad. Sci. U.S.A.* **1996**, *93*, 8362−8367.
(13) Ben-Nun, M.; Martinez, T. J. *Ab initio* quantum molecular dynamics. *Adv. Chem. Phys.* **2002**, *121*, 439−512.
(14) Ben-Nun, M.; Quenneville, J.; Martínez, T. J. *Ab initio* multiple spawning: Photochemistry from first principles molecular dynamics. *J. Phys. Chem. A* **2000**, *104*, 5161−5175.
(15) Heller, E. J. Frozen Gaussians: A very simple semiclassical approximation. *J. Chem. Phys.* **1981**, *75*, 2923−2931.
(16) Yarkony, D. R. Diabolical conical intersections. *Rev. Mod. Phys.* **1996**, *68*, 985−1013.
(17) Robb, M. A.; Bernardi, F.; Olivucci, M. Conical intersections as a mechanistic feature of organic photochemistry. *Pure Appl. Chem.* **1995**, *67*, 783−789.
(18) Klessinger, M.; Michl, J. *Excited States and Photochemistry of Organic Molecules*; VCH Publishers: New York, 1995.
(19) Turro, N. J. *Modern Molecular Photochemistry*; Benjamin/Cummings: Menlo Park, CA, 1978.
(20) Roos, B. O. In *Advances in Chemical Physics: Ab Initio Methods in Quantum Chemistry II*; Lawley, K. P., Ed.; John Wiley and Sons Ltd., 1987; pp 399−445.
(21) Roos, B. O. Theoretical studies of electronically excited states of molecular systems using multiconfigurational perturbation theory. *Acc. Chem. Res.* **1999**, *32*, 137−144.
(22) Ben-Nun, M.; Martínez, T. J. *Ab initio* molecular dynamics study of cis−trans photoisomerization in ethylene. *Chem. Phys. Lett.* **1998**, *298*, 57−65.
(23) Ben-Nun, M.; Martínez, T. J. Photodynamics of ethylene: *Ab initio* studies of conical intersections. *Chem. Phys.* **2000**, *259*, 237−248.
(24) Quenneville, J.; Ben-Nun, M.; Martínez, T. J. Photochemistry from first principles: Advances and future prospects. *J. Photochem. Photobiol. A* **2001**, *144*, 229−235.
(25) Salem, L. The sudden polarization effect and its possible role in vision. *Acc. Chem. Res.* **1979**, *12*, 87−92.
(26) Farmanara, P.; Stert, V.; Radloff, W. Ultrafast internal conversion and fragmentation in electronically excited C2H4 and C2H3Cl molecules. *Chem. Phys. Lett.* **1998**, *288*, 518−522.
(27) Ben-Nun, M.; Martínez, T. J. Electronic absorption and resonance raman spectroscopy from *ab initio* quantum molecular dynamics. *J. Phys. Chem. A* **1999**, *103*, 10517−10527.
(28) Baeck, K. K.; Martinez, T. J. *Ab initio* molecular dynamics with equation-of-motion coupled-cluster theory: Electronic absorption spectrum of ethylene. *Chem. Phys. Lett.* **2003**, *375*, 299−308.
(29) Toniolo, A.; Ben-Nun, M.; Martínez, T. J. Optimization of conical intersections with floating occupation semiempirical configuration interaction wave functions. *J. Phys. Chem. A* **2002**, *106*, 4679−4689.
(30) Quenneville, J.; Martínez, T. J. *Ab initio* study of cis−trans photoisomerization in stilbene and ethylene. *J. Phys. Chem. A* **2003**, *107*, 829−837.
(31) Ko, C.; Levine, B.; Toniolo, A.; Manohar, L.; Olsen, S.; Werner, H.-J.; Martinez, T. J. *Ab initio* excited-state dynamics of the photoactive yellow protein chromophore. *J. Am. Chem. Soc.* **2003**, *125*, 12710−12711.
(32) Molnar, F.; Ben-Nun, M.; Martínez, T. J.; Schulten, K. Characterization of a conical intersection between the ground and first excited state for a retinal analog. *J. Mol. Struct.* **2000**, *506*, 169−178.
(33) Pebay-Peyroula, E.; Rummel, G.; Rosenbusch, J. P.; Landau, E. M. X-ray structure of bacteriorhodopsin at 2.5 Å from microcrystals grown in lipidic cubic phases. *Science* **1997**, *277*, 1676−1681.
(34) Palczewski, K.; Kumasaka, T.; Hori, T.; Behnke, C. A.; Motoshima, H.; Fox, B. A.; Le Trong, I.; Teller, D. C.; Okada, T.; Stenkamp, R. E.; Yamamoto, M.; Miyano, M. Crystal structure of rhodopsin: A G protein-coupled receptor. *Science* **2000**, *289*, 739−745.
(35) Dewar, M. J. S.; Zoebisch, E. G.; Healy, E. F.; Stewart, J. J. P. Development and use of quantum mechanical molecular models. 76. AM1: A new general purpose quantum mechanical molecular model. *J. Am. Chem. Soc.* **1985**, *107*, 3902.
(36) Warshel, A.; Levitt, M. Theoretical studies of enzymic reactions. *J. Mol. Biol.* **1976**, *103*, 227−249.
(37) Gao, J. L. Hybrid quantum and molecular mechanical simulations: An alternative avenue to solvent effects in organic chemistry. *Acc. Chem. Res.* **1996**, *29*, 298−305.
(38) Brooks, B. R.; Bruccoleri, R. E.; Olafson, B. D.; States, D. J.; Swaminathan, S.; Karplus, M. CHARMM: A program for macromolecular energy, minimization, and dynamics calculations. *J. Comput. Chem.* **1983**, *4*, 187−217.
(39) Weiner, P. K.; Kollman, P. A. AMBER: Assisted model building with energy refinement. A general program for modeling molecules and their interactions. *J. Comput. Chem.* **1981**, *2*, 287−303.
(40) Toniolo, A.; Granucci, G.; Martinez, T. J. Conical intersections in solution: A QM/MM study using floating occupation semiempirical configuration interaction wave functions. *J. Phys. Chem. A* **2003**, *107*, 3822−3830.
(41) Toniolo, A.; Olsen, S.; Manohar, L.; Martinez, T. J. Conical intersection dynamics in solution: The chromophore of green fluorescent protein. *Faraday Discuss.* **2004**, *127*, 149−163.
(42) Mandal, D.; Tahara, T.; Meech, S. Excited-state dynamics in the green fluorescent protein chromophores. *J. Phys. Chem. B* **2004**, *108*, 1102−1108.
(43) Dang, L. X.; Pettitt, B. M. Simple intermolecular model potentials for water [SPC and TIP3P]. *J. Phys. Chem.* **1987**, *91*, 3349−3354.
(44) Humphrey, W. F.; Dalke, A.; Schulten, K. VMD−Visual molecular dynamics. *J. Mol. Graphics* **1996**, *14*, 33.

AR040202Q